

# PERFORMANCE EVALUATION OF CEMENT MORTAR AND CONCRETE WITH INCORPORATED MICRO FILLERS OBTAINED BY COLLISION MILLING IN DISINTEGRATOR

#GIRTS BUMANIS\*, DIANA BAJARE\*, DMITRI GOLJANDIN\*\*

\*Institute of Materials and Structures, Riga Technical University, Latvia

\*\*Department of Materials Engineering, Tallinn University of Technology, Estonia

#E-mail: girts.bumanis@rtu.lv

Submitted February 14, 2017; accepted April 10, 2017

**Keywords:** Collision milling, Disintegration, Quartz and limestone sand, Cement mortar, High strength self-compacting concrete

*This research focuses on natural quartz and natural quartz-limestone sand mechanoactivation with the high energy milling by collision in disintegrator using different energy rates (8.4 and 25.2 kWh·t<sup>-1</sup>) and its application effectiveness as microfiller in Portland cement composites. The obtained microfiller was used to partially replace sand in mortar and to partially replace cement in high performance self-compacting concrete (SCC). The activity factor of disintegrated microfillers in time was investigated to detect the potential changes of sand particle properties during milling and the subsequent storage. XRD, BET, morphological investigation and grading analysis was performed for disintegrated sand. Mechanical, physical and durability properties regarding to chloride penetration and freeze-thaw resistance were determined to prepared cement composites. The results indicate that cement mortar which was prepared with disintegrated microfillers right after their disintegration provides compressive strength increase up to 20 % comparing to the reference mixture and the time factor has significant effect on the activity of disintegrated sand. The SCC strength slightly decreased, if cement was replaced by the disintegrated sand up to 15 wt. %, while the results of durability test indicate that resistance to freeze-thaw damage and chloride penetration could remain in the level of the reference mixture.*

## INTRODUCTION

The main qualities characterising mineral additives in cement composites are purity and stability of chemical composition, particle grading properties and shape factor. To obtain powder mineral additives milling is often used to reduce particle size distribution and morphology of the particles. Traditionally ball and planetary ball milling is applied, however, this method has its fair share of shortcomings: the difficult construction and high metal consumption, great wear of grinding parts, the product is exposed to intense heat, etc. Grinding by collision is more effective method for refining of brittle material and an alternative for the mills that produce mineral supplements for construction mixtures. This method is referred as disintegrator technology, where the material is milled not as a result of low-speed impact abrasion but rather as the result of a highly effective high-speed and high-intensity impact [1]. The main kinetic parameter in the processing of a material in disintegrators is the specific energy ( $E_s$ ) of treatment in kJ·kg<sup>-1</sup> or kWh·t<sup>-1</sup>, important both from the point of view of the grinding effect (grindability) and the economic aspect of the process. The rotation speed of grinding elements is regarded as one of the most important factors. Unlike ball and planetary mills, disintegrator mills have a rather

simple construction. Instead of many grinding details, it has two rotors with grinding elements, which revolve in opposite directions at high speed. A particle accelerated by the first rotor is sent into the opposing rotor. The relative velocity of the collision could occur at up to 200 m·s<sup>-1</sup> and beyond. The tensions generated in the particle during this impact may significantly surpass its tensile strength. The disintegration process is very short, and takes up a fraction of a second. Another benefit is the high quality of the blending of the processed components in the mixture, a process that could be performed simultaneously with the milling.

During the disintegration of the particles a new surface area is formed, which has not had time to oxidise and therefore could be extremely chemically active. This is called mechanical activation, which results in enhanced reactivity of solids due to physicochemical changes induced by milling [2]. Nikashina et al. has reported that in the milling of natural zeolites with energy rate below 0.5 - 0.7 kJ·g<sup>-1</sup> the dominant process is disintegration of zeolite particles and changes in bulk density while in the milling with higher energy input amorphous phase prevails [3]. Gbureck et al. reported that prolonged high-energy ball milling of  $\beta$ -tricalcium phosphate led to mechanically induced phase transformation from the crystalline to the amorphous state resulting in the

thermodynamic solubility increase up to nine times and accelerated the normally slow reaction with water and such cements could reach the compressive strength up to 50 MPa [4]. The high-energy ball milling of clay minerals results in the decrease of the particle size (i); in significant increase of the specific surface area (ii); cation exchange capacity values (iii), and in the exposure of new, amphoteric surfaces, significantly changing the electrophoretic mobility while prolonged milling produced amorphous alumina-silicate aggregates (iv) [5]. Terada and Yonemochi indicated that the disintegration time of talc lead to decrease of the average particle size and increase of the specific surface area and also polar part of surface energy was increased by 41 % and hydrophilic surface was indicated [6]. Cao et al. reported that high energy ball milling of boiler bottom slag destroys crystal phase of mullite and quartz and Al–O–Si and Si–O–Si bonds are fractured, while amorphous  $\text{Al}_2\text{O}_3$  and  $\text{SiO}_2$  phase increase, which improves slag activity [7]. The amorphous materials containing  $\text{SiO}_2$  often has pozzolanic activity which is beneficial for Portland cement based materials [8]. The milling time of coal combustion bottom ash in planetary ball mill increase the activity of obtained microfiller; therefore cement could be replaced by the amount from 20 to 40 % [9]. Such mechanical activation could be applied in wide range of industries including construction industry, where fine graded amorphous mineral materials could be used as supplementary cementitious materials or pozzolanic materials to increase the strength of cement based composites [10]. If high energy milling using disintegrator could activate quartz sand enhancing hardening processes in cement composites, which leads to higher compressive strength, then this would be beneficial for the concrete industry and would provide alternative method for obtaining effective reactive microfiller.

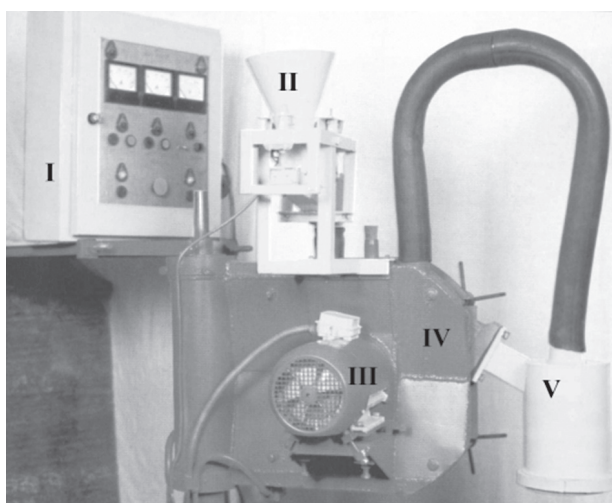


Figure 1. Semi-industrial disintegrator milling system DSL-115 with direct operating system.

This research focuses on natural quartz and natural quartz-limestone sand mechanoactivation with the high energy milling by collision in disintegrator using different energy rates (8.4 and 25.2  $\text{kWh}\cdot\text{t}^{-1}$ ). Obtained material was evaluated on its application effectiveness as microfiller in Portland cement composites as partial sand replacement (10 wt. %) in cement mortars and as partial cement replacement (5 - 15 wt. %) in high strength self compacting concrete.

## EXPERIMENTAL

### Experimental Methods

Semi-industrial disintegrator milling system DSL-115 with direct operating system (disintegrator) was used for collision milling of selected sand (Figure 1). Disintegrator consists of control panel (I), feeding system (II), two electrical motors (III), rotors (IV) and output channel (V). Maximum size of feed material – 12 mm, maximum diameter of rotors – 480 mm, nominal power – 9.5 kW, the rotation velocity of rotors was up to 3000 rpm, the impact velocity was up to  $150\text{ m}\cdot\text{s}^{-1}$ . In this research natural quartz sand and natural mixed quartz and limestone sand were disintegrated and tested.

The particle size distribution was carried out on the vibratory sieve shaker Analysette 3 PRO for fractures between 0.05 - 2 mm and on the laser diffraction particle sizer Analysette 22 Compact for fractures  $< 50\text{ }\mu\text{m}$ . The morphology of obtained powder material was described with scanning electron microscope (SEM) Tescan Mira/LMU. The specific surface area (BET) was determined by ESA analysis using of PSKh instrument. In the experiments with cement composites Portland cement CEM I 42.5 N produced by Cemex Ltd (Latvia) characterized with oxide composition:  $\text{SiO}_2$  – 18.8 %,  $\text{Al}_2\text{O}_3$  – 3.9 %,  $\text{Fe}_2\text{O}_3$  – 3.0 %,  $\text{CaO}$  – 63.2 %,  $\text{MgO}$  – 3.2 %,  $\text{K}_2\text{O}$  – 1.1 %,  $\text{Na}_2\text{O}$  – 0.2 %,  $\text{Na}_2\text{O}_{\text{ekv}}$  – 0.9 %, mineral composition  $\text{C}_3\text{S}$  – 57.7 %,  $\text{C}_2\text{S}$  – 18.2 %,  $\text{C}_3\text{A}$  – 6.4 %,  $\text{C}_4\text{AF}$  – 9.8 %, free lime 2.0 % and Blaine fineness of  $3787\text{ cm}^2\cdot\text{g}^{-1}$  was used. Particle size distribution is given in Figure 3.

The disintegrated sand reactivity regarding to milling energy and storage time was assessed in cement mortar where sand was partial replaced (10 wt. %) with obtained microfiller. Two milling energy rates (8.4 and 25.2  $\text{kWh}\cdot\text{t}^{-1}$ ) were applied to the sand. The disintegrated sands were applied to the cement mortar mixture immediately after disintegration (0 days), then after 2 days the mixing procedure was repeated with 2 day old disintegrated sand (2 days) and finally the same procedure was repeated after 28 days of disintegration (28 days). The mixing procedure of cement mortar included mixing all dry components together for 1 minute using electrical one shaft hand mixer. Then the calculated amount of water with superplasticizer was added to the mixture and mixing was continued until homogenous mixture has



been prepared. The consistence of fresh mortars (by flow table) was determined according to LVS EN 1015-3. The prepared mortar mixtures were cast in 40×40×160 mm prismatic moulds. The compressive strength of the hardened mortar was tested according to LVS EN 196-1 at the age of 7 days, 28 days and 360 days.

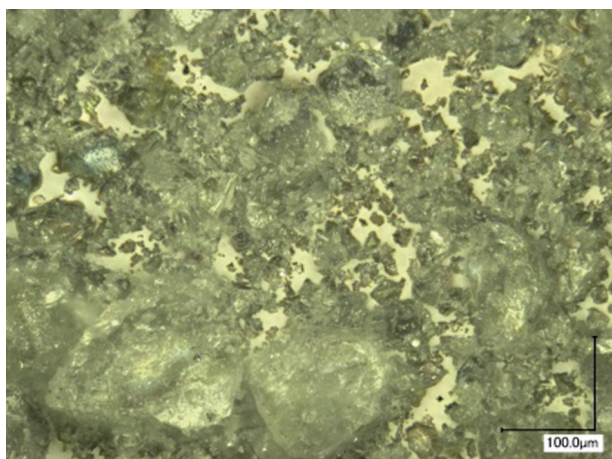
After the experiments with cement mortar, the disintegrated sand treated with specific milling energy ( $E_s$ ) 8.4 kWh·t<sup>-1</sup> was introduced in the high strength self-compacting concrete (SCC) to partially replace cement by 5, 10 and 15 wt. % respectively. The mixing procedure was carried out in a planetary drum mixer and included



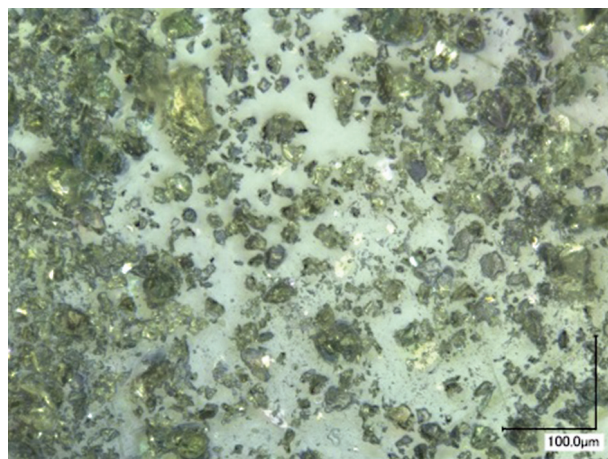
a) untreated QS



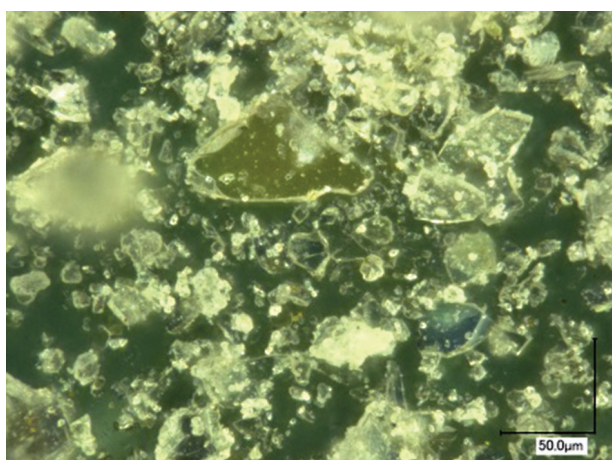
d) untreated MS



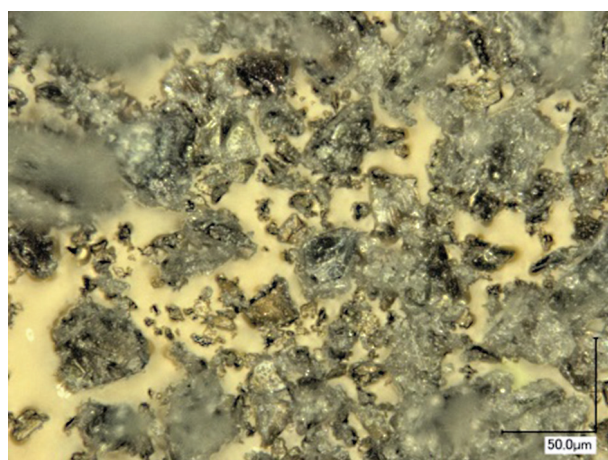
b) disintegrated at 8.4 kWh·t<sup>-1</sup> QS



e) disintegrated at 8.4 kWh·t<sup>-1</sup> MS



c) disintegrated at 25.2 kWh·t<sup>-1</sup> QS



f) disintegrated at 25.2 kWh·t<sup>-1</sup> MS

Figure 2. Morphology of the tested sand: natural quartz sand QS: a) untreated, b) disintegrated at 8.4 kWh·t<sup>-1</sup>; c) disintegrated at 25.2 kWh·t<sup>-1</sup>; natural quartz-limestone sand MS: d) untreated, e) disintegrated at 8.4 kWh·t<sup>-1</sup>; f) disintegrated at 25.2 kWh·t<sup>-1</sup>.

the following stages: all dry components were mixed together for 120 s to obtain homogenous mixture of dry components. Then half of the calculated amount of water was added and mixing was continued for another 120 s. The remaining water with superplasticizer was added and mixing was continued for additional 120 s. Finally, density of fresh concrete was measured according to LVS EN 12350-6 and workability of SCC was tested according to LVS EN 12350-8. The samples were casted in  $100 \times 100 \times 100$  mm moulds for further investigation. The compressive strength was determined according to LVS EN 12390-3. Three specimens at every age were tested and average value with deviation was calculated.

Durability of the chloride penetration was performed according to NT BUILD 492. Three specimens with

$\varnothing 100$  mm and height 50 mm were created and tested. The freeze-thaw resistance of SCC was performed according to the CDF to test the capillary suction of de-icing solution and freeze (RILEM TC 117-FDC). Six specimens of each series were tested. 3 % NaCl solution was used as deicing solution.

#### Raw sand properties

Pure natural washed quartz sand with fraction  $< 1$  mm (QS) and natural washed quartz-limestone sand with fraction 0.3/2.5 mm was tested (MS) (Particle size distribution is given in Figure 3). Both sand types come from quarry Saulkalne-S (Latvia) and corresponds to LVS EN 13139 "Aggregates for mortar". The chemical composition of selected sands is given in Table 1. QS and MS contained particles  $< 0.125$  mm below 0.3 wt. %. The physical and mechanical properties of main minerals in tested sands are given in Table 2. Two sand collision milling regimes were applied in disintegrator with  $E_s$  8.4 and 25.2 kWh·t<sup>-1</sup>, which was assessed by number of times the sand was disintegrated through the milling system (1 and 3 times respectively). The designation of disintegrated sand was selected according to the applied  $E_s$  treatment (QS8.4; QS25.2; MS8.4 and MS25.2).

#### Mortar mixture composition

The cement mortar was prepared according to mixture compositions given in Table 3. Cement to sand ratio of reference mixture (CTR) was 1:2. QS and MS sand ratio in mixture composition was 1:1. The water to cement ratio was constant for all mixtures and it was 0.4. The superplasticizer was added in the proportion of 0.425 wt. % from the amount of cement. 20 wt. % of QS or MS from mixture design was disintegrated and integrated in mortar composition, therefore the disintegrated sand partially replaced natural sand (10 wt. % from total amount of sand).

Table 1. Chemical composition of selected sand.

Chemical component	Content, wt. %	
	QS	MS
SiO <sub>2</sub>	96.8	72.5
Al <sub>2</sub> O <sub>3</sub>	1.4	5.2
Fe <sub>2</sub> O <sub>3</sub>	0.3	1.2
CaO	0.3	14.6
MgO	0.2	2.2
Na <sub>2</sub> O	–	1.2
K <sub>2</sub> O	–	2.8
SO <sub>3</sub>	–	0.2
LOI, 1000°C	0.3	5.6

Table 2. Physical and mechanical properties of main minerals in tested sands.

Property	Limestone (in MS)	Quartz sand (QS)
Specific Gravity (g cm <sup>-3</sup> )	2.5-2.7	2.8-2.9
Mohs Hardness	3-4	7
Compressive strength (MPa)	60-170	200-250

Table 3. Mixture composition of prepared mortar with disintegrated sand.

Component	Mixture composition (mass ratio)				
	CTR	Q8	Q25	M8	M25
Cement Cemex CEM I 42.5N	1	1	1	1	1
QS	1	0.8	0.8	1	1
MS	1	1	1	0.8	0.8
QS8.4	–	0.2	–	–	–
QS25.2	–	–	0.2	–	–
MS8.4	–	–	–	0.2	–
MS25.2	–	–	–	–	0.2
Water	0.4	0.4	0.4	0.4	0.4
Superplasticizer (%)*	0.425	0.425	0.425	0.425	0.425
Workability (Ø, mm)	230	210	200	190	200

\* from the weight of cement



### High strength self-compacting concrete mixture composition

Several SCC mixture series were created with different amount of disintegrated QS and MS sand (treated with  $E_s$  8.4 kWh·t<sup>-1</sup>) as partial cement replacement (from 5 to 15 wt. %), and mixture compositions are given in Table 4. Reference (REF) mixture composition contains 500 kg·m<sup>-3</sup> cement. Natural washed gravel with fraction 4/12 mm was used as a coarse filler and natural washed sand with fraction 0.3/4 mm was used as a fine filler. The quartz sand with fraction < 0.3 mm was used as extra fine filler to improve workability of the SCC and avoid segregation of fresh mixture (grading analysis of raw materials is given in Figure 3). The water to cement with disintegrated sand (DS) ratio (W/(C+DS)) was constant for all mixture compositions being 0.38. The workability of SCC remained constant by changing the amount of superplasticizer and the cone flow remained > 600 mm.

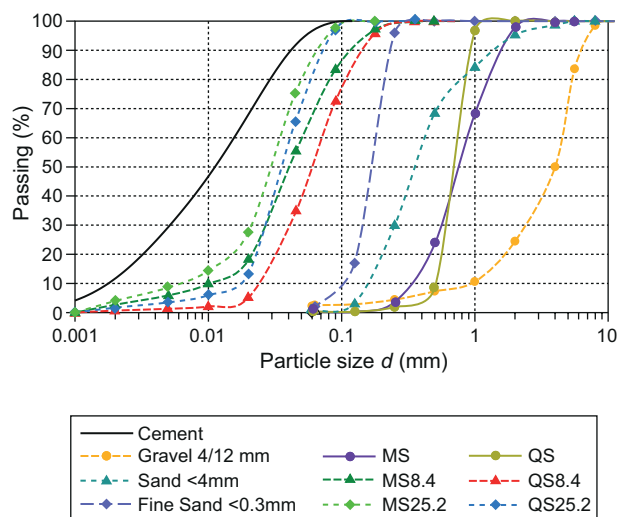


Figure 3. Cumulative particle size distribution raw materials for cement composites and disintegrated sand at different energy rates.

## RESULTS AND DISCUSSION

### Properties of disintegrated sand

The morphology of untreated and treated QS and MS is given in Figure 2. The untreated QS has transparent clearly visible quartz particles with smoothened and rounded shape defined by QS natural occurrence and treatment during processing (Figure 2a), while in MS in addition to the quartz particles smooth limestone particles were detected (Figure 2d). The preliminary milling with  $E_s$  8.4 kWh·t<sup>-1</sup> effectively reduced the size of MS particles (Figure 2e), while for the QS beside fine particles coarser particles with size > 0.1mm was identified (Figure 2b). The sand milling with  $E_s$  25.2 kWh·t<sup>-1</sup> effectively reduced the size of coarser particles of QS (Figure 2c) and sand was more homogenous in its structure similar to MS while milling with increased  $E_s$  did not change particle structure significantly for MS.

The particle size analysis after collision milling using disintegrator is given in Table 5 and Figure 2. The overall tendency was that  $d$  values of the disintegrated sand reduces in particle size with the increase of milling  $E_s$ . After collision milling of QS with energy  $E_s$  8.4 kWh·t<sup>-1</sup> the  $d_{10}$  value was 24.5  $\mu$ m (QS8.4) and by increasing the milling energy to  $E_s$  25.2 kWh·t<sup>-1</sup> (QS25.2) the  $d_{10}$  value reduced from 17.7  $\mu$ m. For MS the  $d_{10}$  reduced from 10.0 to 6.0  $\mu$ m (MS8.4 and MS25.2). The median particle value ( $d_{50}$ ) reduced from 59.7 to 35.6  $\mu$ m for QS while for MS the  $d_{50}$  value reduced from 40.5 to 30.0  $\mu$ m by

Table 5.  $d_{10}$ ,  $d_{50}$  and  $d_{90}$  values of disintegrated sand.

Sample	$d_{10}$ ( $\mu$ m)	$d_{50}$ ( $\mu$ m)	$d_{90}$ ( $\mu$ m)
QS*	~200	~400	~700
MS*	~500	~1200	~2000
QS8.4	24.5 $\pm$ 0.2	59.7 $\pm$ 1.2	141.0 $\pm$ 1.4
QS25.2	17.7 $\pm$ 0.6	35.6 $\pm$ 0.4	71.5 $\pm$ 1.4
MS8.4	10.0 $\pm$ 0.9	40.5 $\pm$ 1.9	116.5 $\pm$ 2.2
MS25.2	6.0 $\pm$ 0.2	30.0 $\pm$ 0.5	64.7 $\pm$ 2.8

\* determined by sieve analysis

Table 4. Mixture composition of high strength self-compacting concrete.

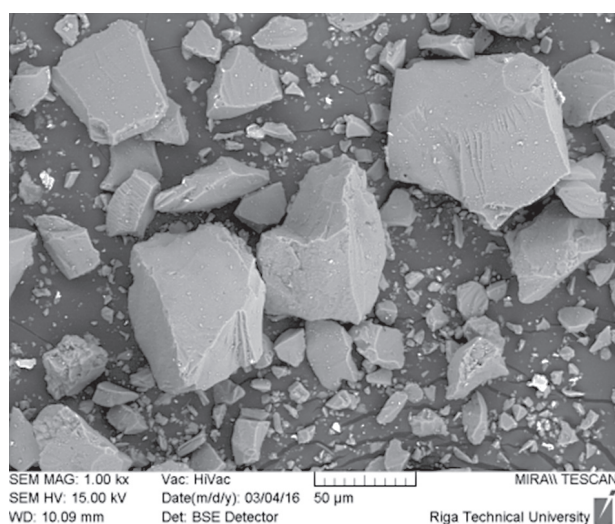
Component	Mixture design (kg·m <sup>-3</sup> )						
	REF	C5Q	C10Q	C15Q	C5M	C10M	C15M
Cement Cemex CEM I 42.5N	500	475	450	425	475	450	425
Sand 0.3/4mm	700	700	700	700	700	700	700
Fine Sand < 0.3mm	118	118	118	118	118	118	118
Gravel 4/12 mm	908	908	908	908	908	908	908
Water	190	190	190	190	190	190	190
Superplasticizer	4.0	4.0	4.0	4.0	4.0	4.0	4.0
Disintegrated sand (QS8)	—	25	50	75	—	—	—
Disintegrated sand (MS8)	—	—	—	—	25	50	75
W/C	0.38	0.40	0.42	0.45	0.40	0.42	0.45
W/(C+DS)	0.38	0.38	0.38	0.38	0.38	0.38	0.38

increasing milling  $E_s$  from 8.4 to 25.2 kWh·t<sup>-1</sup>. The  $d_{90}$  value shows the particle size reduction from 141.0 µm to 71.5 µm for QS and from 116.5 µm to 64.7 for MS. The laser grading analysis shows that MS25.2 has the finest particle size, if the applied collision milling energy was  $E_s$  25.2 kWh·t<sup>-1</sup> followed by MS8.4 and Q25.2.

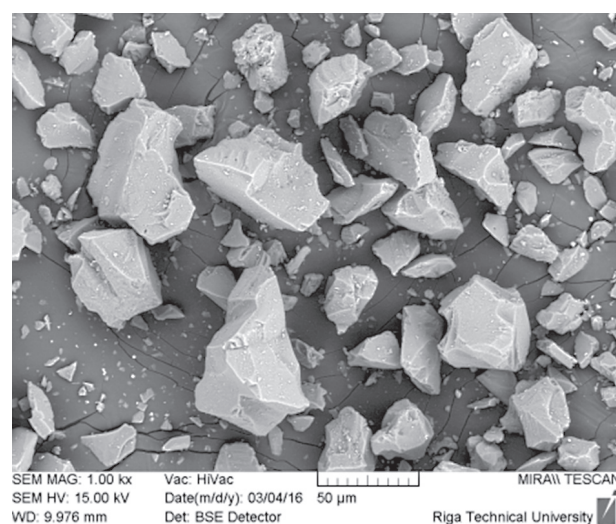
SEM analysis confirms the results of laser grading analysis and indicates that the coarsest particles have been disintegrated by the increase of milling  $E_s$  (Figure 3). The QS after disintegration have particles with plate-like structure with smooth surface. The collision of particles in disintegrator splits the particle creating layered pieces which could possess reactivity due to the mechanoactivation and formation of new surfaces due to the bond breakage. The disintegrated MS (Figure 4c and d) have smaller particles compared to QS which could be associated with the mechanical strength and physical properties of the particles (Table 2). Two

types of particles can be divided: particles with smooth surface, which are referred as quartz particles, and particles with rough surface, referred as limestone. In further investigations smooth (QS) or rough (MS) surface particle morphology could affect the workability, physical and durability properties of cement composites regarding to particle water demand and water absorption with related influence on durability.

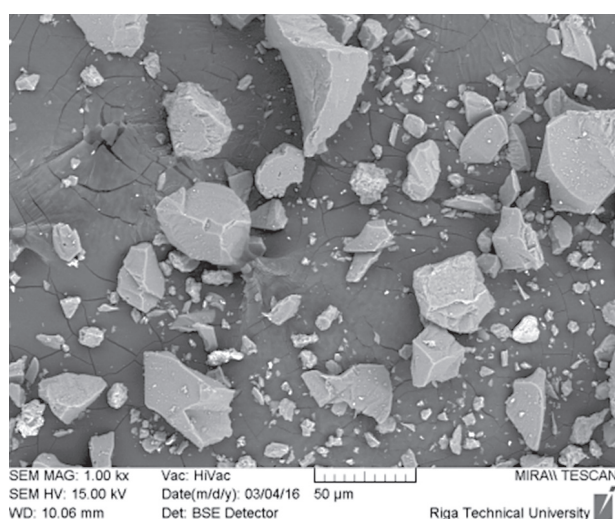
The results of the grindability expressed as the medium size of particles ( $d/d_0$ ), and the ratio of specific surface areas of the ground powders and initial sands ( $A/A_0$ ) is given in Figure 5. The particle size reduction comparing QS and MS was more efficient for MS which contained quartz and limestone particles. Higher milling energy  $E_s$  was necessary to reduce the size of QS particles with  $d_{10}$  below 10µm. The difference in applied  $E_s$  to reduce particle size is explained by the differences in mechanical properties QS and MS (Table 2).



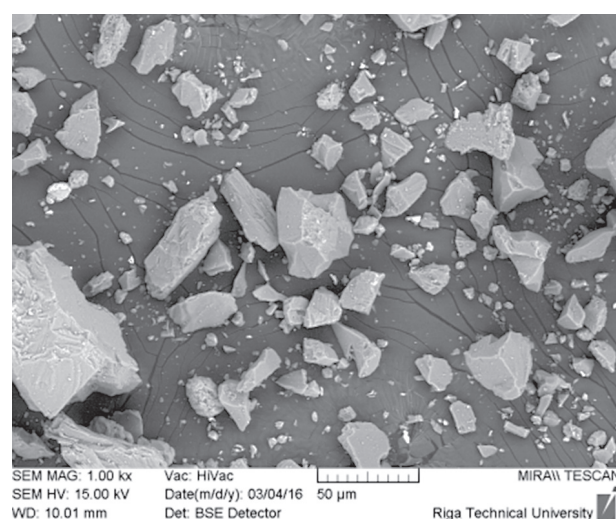
a) QS8.4



b) QS25.2



c) MS8.4



d) MS25.2

Figure 4. Morphology of disintegrated sand. Sand disintegrated with:  $E_s$  8.4 kWh·t<sup>-1</sup>: a) quartz sand (QS8.4), c) quartz-limestone sand (MS8.4);  $E_s$  25.2 kWh·t<sup>-1</sup>: b) quartz sand (QS25.2), d) quartz-limestone sand (MS25.2).

The density of selected sand was nearly equal but hard and durable QS sand takes longer to grind; therefore the size reduction of softer and less durable MS is much more immediate. Similarly, the  $S_{\text{BET}}$  of MS increases faster than that of QS (Table 6). The dependence of the obtained material surface area on the applied  $E_s$  during collision milling was shown in the Table 6. It was concluded that the increase of  $E_s$  from 8.4 to 25.2 kWh·t<sup>-1</sup> was not practically or economically useful for MS particles while for QS the increase of  $E_s$  continued to reduce particle size with a linear curve.

The potential mechanoactivation or phase change of QS was evaluated with the XRD. XRD results indicate that no amorphisation or phase change was present and the same phases with similar intensity both for raw QS and QS25.2 tested right after disintegration (QS25.2\_0d)

Table 6. Specific surface area  $S_{\text{BET}}$  of natural and disintegrated sand.

Sample	Specific surface area (cm <sup>2</sup> ·g <sup>-1</sup> )		
	Initial	8.4 kWh t <sup>-1</sup>	25.2 kWh·t <sup>-1</sup>
QS	< 50	665	2716
MS	< 30	2553	3571

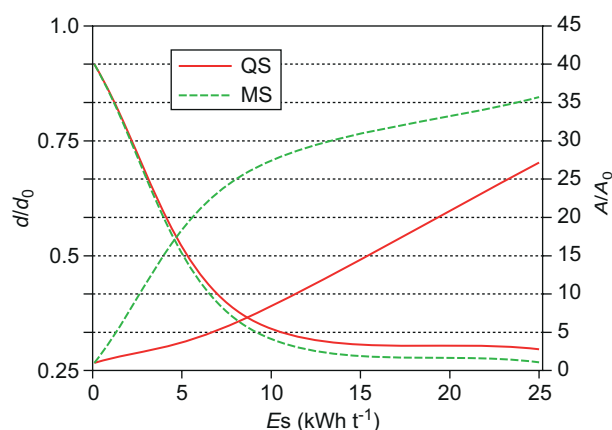


Figure 5. Dependence of the ratio of median size  $d$  from the initial median size  $d_0$  and the ratio of specific area  $A$  depending on its initial value  $A_0$  and the specific energy of grinding.

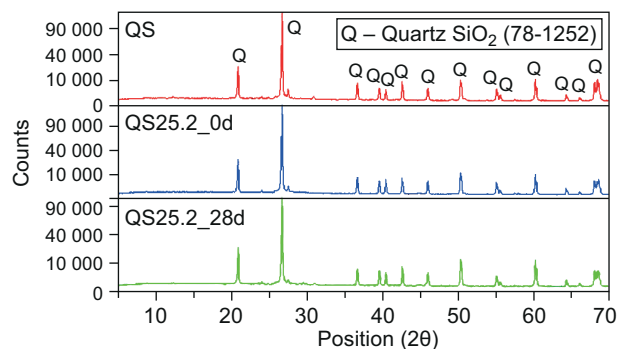


Figure 6. Diffractogram of raw quartz sand and quartz sand after high energy milling in disintegrator.

and at the 28<sup>th</sup> day after disintegration (QS25.2\_28d) was present (Figure 6). Therefore with the increase of milling  $E_s$  only particle size reduction and re-homogenization has taken place.

#### Disintegrated sand in cement mortar

The decrease of fresh mortar workability from 230 mm for reference mixture CTR to 190 - 210 mm was observed as the disintegrated sand replaced natural sand in mixture composition by 10 wt. % (Table 3). This was related to the fine nature of the obtained microfiller which was obtained after disintegration and introduced in the mixture composition; therefore higher particle surface attracts more water from the cement paste slightly reducing its workability. The compressive strength for CTR sample was 58 MPa at the age of 7 days, 64 MPa at 28 days and 85 MPa at 365 days. The compressive strength index (CSI) in % was calculated for better comparison between the cement mortars mixtures prepared after different periods of time comparing the CTR strength at the respective ages (Figure 7).

#### Compressive strength index of cement mortars at early age

It was found out that the age of disintegrated sand application in cement mortar was essential for the high strength gain. The immediate application of disintegrated sand in cement mortar mixture (results under index 0d in Figure 7) increased early CSI (7 days) up to 111 % and 114 % for Q8 and Q25, while for the mortar prepared with MS CSI increased to 104 % and 109 % (M8 and M25). The effectiveness of sand as microfiller reduced, when mortar was prepared with 2 days old disintegrated sand (the results under index 2d in Figure 7). The CSI reduced to 99 % for Q8, while for Q25 slight increase of strength was observed - 104 % respectively. For the samples with MS the strength increase was from 102 to 106 % (M8 and M25). The prolonged storage of disintegrated sand up to 28 days decreased CSI even more comparing to CTR (the results under index 28d in Figure 7). For the mixture composition Q8 it was 96 %, M8 – 97 %, M25 – 99 % respectively. Slight SCI increase was observed only for Q25 – up to 103 %. The strength reduction after storage period could be explained by the reduction of activity of disintegrated sand and the reactive microfiller turning into the dust which traditionally deteriorates cement composite properties. High early strength with fresh disintegrated sand could also be contributed to the active crystallization centers in fresh mortar paste, therefore higher strength gain was achieved. The immediate application of sand after disintegration has loosened the bulk of sand powder particles therefore it disperses evenly easily in the mortar paste while stored sand has compacted and the mixing and homogenization was less effective which finally donated to the compressive strength development.



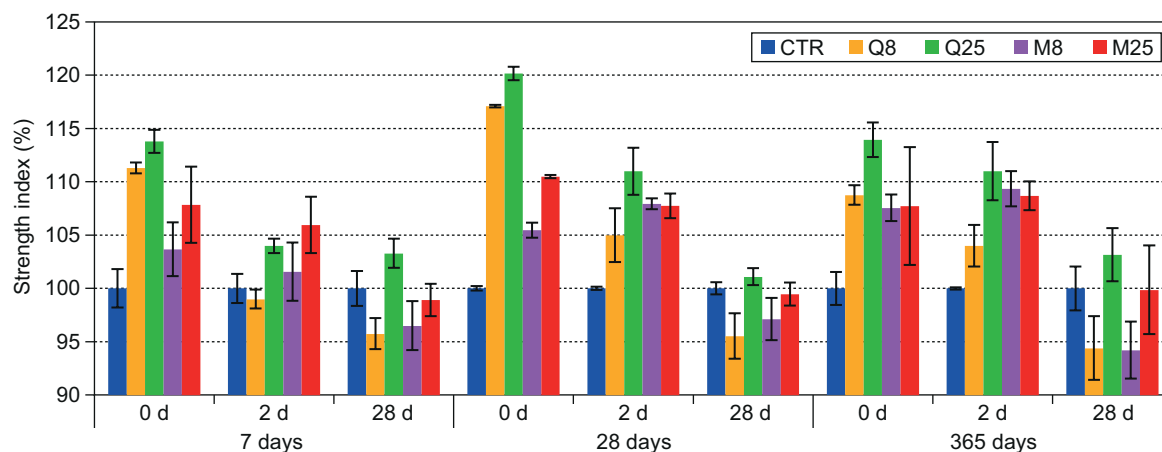


Figure 7. Compressive strength index (%) of cement mortar at the age of 7 days made with 0, 2 and 28 day old sand after disintegration.

#### *Compressive strength index of cement mortar at 28 days*

Similar tendencies can be observed for cement mortar at the age of 28 days (Figure 7). With instantly used disintegrated QS (0 days) the CSI increased to 117 and 120 % for mixture composition Q8 and Q25 comparing to CTR. For mixtures M8 and M25 CSI increased to 105 and 110 % and proved to be less effective. The mortar samples prepared after 2 days of sand disintegration provided lower CSI comparing to the mortar samples prepared after 0 days; however, the results were higher comparing to CTR: 105 % and 111 % for Q8 and Q25 and 108 % for both M8 and M25. The mortar prepared with 28 days old disintegrated sand showed decrease of CSI in most cases, similar to the mortar properties at the age of 7 days. The CSI reduced from 96 to 99 % for all cases except for samples Q25, which remained similar to CTR (101 %).

#### *Long term (365 day) compressive strength index of cement mortar*

The compressive strength results at 365 days confirm the importance of time factor on disintegrated sand properties in cement mortars. Instantly used disintegrated sand increase long term CSI from 109 to 114 % for Q8 and Q25 and around 108 % for M8 and M25 comparing to CTR. The cement mortars with 2 day old disintegrated sand had CSI increase from 104 to 111 % for Q8 and Q25 and 109 % both for M8 and M25.

The increase of milling energy has a noticeable effect on duration of sand microfiller effectiveness in cement mortar. The milling energy effect on instant application of disintegrated sand had negligible effect while at the age of 2 and 28 days difference is noticeable.

Regarding the positive effect of instantly disintegrated sand on mortar compressive strength properties, the instantly disintegrated sand was applied in SCC as partial cement replacement to evaluate the possibility and potential to use high energy milled sand application in concrete.

#### *Disintegrated sand instant application in high strength self-compacting concrete*

The properties of fresh SCC are given in Table 7. The density of fresh concrete was  $2423 \text{ kg}\cdot\text{m}^{-3}$  for REF and slightly decreased from 2395 to  $2420 \text{ kg}\cdot\text{m}^{-3}$  as cement was replaced with the disintegrated sand. The workability of fresh SCC expressed as cone flow was  $\varnothing 63 \times 63 \text{ cm}$  for REF and was slightly affected by the disintegrated sand incorporation in the mixture composition similar to cement mortar. The cone flow reduced from  $\varnothing 62 \times 61.5 \text{ cm}$  to  $\varnothing 58 \times 58 \text{ cm}$  except for the mixture composition C15M with cone flow with  $\varnothing 64 \times 65 \text{ cm}$ . The cone flow time remained the same for SCC with disintegrated QS (from 23.2 to 27.1 s), while for SCC with disintegrated MS flow time slightly increased from 28.0 to 33.1 s.

Table 7. Fresh self-compacting concrete (SCC) properties and physical properties of hardened SCC.

Property	REF	C5Q	C10Q	C15Q	C5M	C10M	C15M
Density of fresh concrete ( $\text{kg}\cdot\text{m}^{-3}$ )	$2423 \pm 5$	$2415 \pm 2$	$2398 \pm 5$	$2395 \pm 4$	$2420 \pm 3$	$2405 \pm 5$	$2407 \pm 3$
Cone flow diameter, (mm)	$63 \times 63$	$58 \times 58$	$61.5 \times 62$	$60 \times 60$	$61 \times 61$	$61 \times 61$	$64 \times 65$
Flow time, (s)	25.0	23.2	27.1	24.7	31.6	28.0	33.1
Density of hardened concrete ( $\text{kg}\cdot\text{m}^{-3}$ )	$2280 \pm 3$	$2289 \pm 2$	$2285 \pm 3$	$2280 \pm 7$	$2278 \pm 3$	$2277 \pm 4$	$2270 \pm 8$
Open porosity (vol. %)	$10.7 \pm 0.3$	$9.5 \pm 1.2$	$10.5 \pm 0.4$	$10.3 \pm 0.9$	$11.1 \pm 0.2$	$11.2 \pm 0.5$	$11.3 \pm 0.4$
Water absorption (wt. %)	$4.7 \pm 0.1$	$4.2 \pm 0.8$	$4.6 \pm 0.2$	$4.5 \pm 0.4$	$4.8 \pm 0.1$	$4.9 \pm 0.2$	$5.0 \pm 0.2$



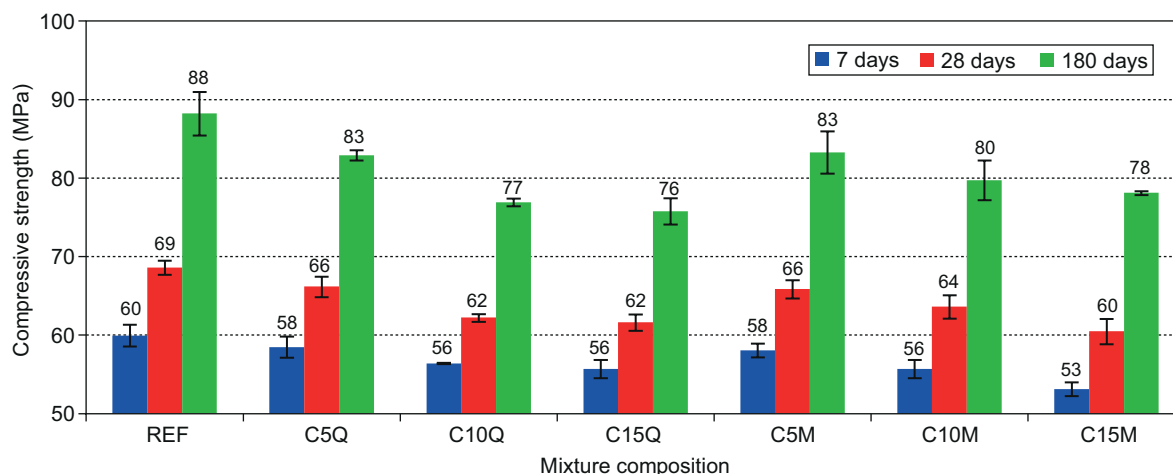


Figure 8. Compressive strength results of self-compacting concrete made with disintegrated sand as partial cement replacement.

The SCC compressive strength results indicate that the partial cement replacement with both types of disintegrated sand reduces SCC strength at 7, 28 and 180 days comparing to the reference mix (REF) (Figure 8). Early compressive strength for REF was 60 MPa at 7<sup>th</sup> day, 69 MPa at 28<sup>th</sup> day and 88 MPa 180<sup>th</sup> day respectively. The 5 wt. % substitution of cement with disintegrated sand reduced the compressive strength to 58; 66 and 83 MPa with no contribution to the selected sand type. The 10 wt. % substitution of the cement with the disintegrated sand resulted in the compressive strength reduction to 56, 62 and 77 MPa for SCC made with QS and 56, 64 and 80 MPa for SCC made with MS. The cement replacement by 15 wt. % reduced the compressive strength to 56, 62 and 77 MPa for SCC made with QS and 53, 60 and 78 MPa to SCC made with MS.

The relative compressive strength comparison by age factor of the SCC and partial cement replacement with disintegrated sand is given in Figure 9. It was found out that 5 wt. % cement replacement with both disintegrated sands reduced the compressive strength

from 97 to 98 % at 7 days and the reduction increased during hardening up to 94 % at 180 days comparing to the REF compressive strength. Similar tendencies were observed also with 10 wt. % and 15 wt. % cement replacement. The aging factor of SCC hardening even increased the difference of compressive strength between REF and SCC with disintegrated sand. Incorporation of the disintegrated sand as partial cement replacement did not provide any positive development with regard to the SCC compressive strength.

#### Freeze-thaw durability

The test results of freeze-thaw durability are given in Figures 10 and 11. It was found that cement replacement by 15 wt. % reduces resistance to freeze-thaw durability significantly. After 14 freeze-thaw cycles the weight loss was from 0.7 to 0.8 kg·m<sup>-2</sup> for both mixture compositions with disintegrated sand (C15Q and C15M). The weight loss increased rapidly between 28 and 56 freeze-thaw cycles and weight loss increased to 7.0 and 7.1 kg·m<sup>-2</sup> respectively. After 56 freeze-thaw

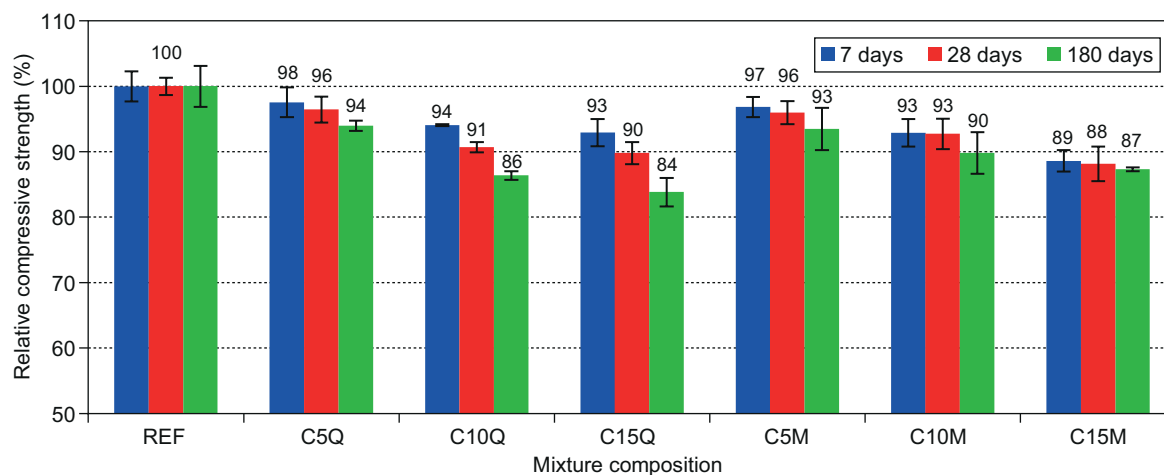


Figure 9. Relative compressive strength of SCC with disintegrated sand as partial cement replacement.

cycles constant weight loss was observed and surface loss reached 19.9 to 20.6 kg·m<sup>-2</sup> after 196 freeze-thaw cycles. Higher resistance to freeze-thaw deterioration was detected for the samples with cement replacement by 10 wt. %. The surface scaling was 0.2 kg·m<sup>-2</sup> after 42 freeze-thaw cycles for C10M and 0.1 kg·m<sup>-2</sup> after 56 freeze-thaw cycles for C10Q. After 84 freeze-thaw cycles rapid increase of surface scaling was observed for C10M, when surface scaling increased from 1.5 kg·m<sup>-2</sup> at 84<sup>th</sup> cycle to 12.2 kg·m<sup>-2</sup> at 196<sup>th</sup> cycle. For the mixture C10Q durability to frost damages was higher and surface scaling increased rapidly only after 98 cycles when the surface scaling increased from 1.0 kg·m<sup>-2</sup> to 8.0 kg·m<sup>-2</sup> after 196 freeze-thaw cycles (Figure 11). More durable SCC regarding to the freeze-thaw resistance was obtained with 5 wt. % substitution of the cement and similar freeze-thaw performance was observed comparing to the REF. Gradual surface scaling increase begun at 56 cycles and after 196 cycles it reached from 3.7 to 4.7 kg·m<sup>-2</sup>.

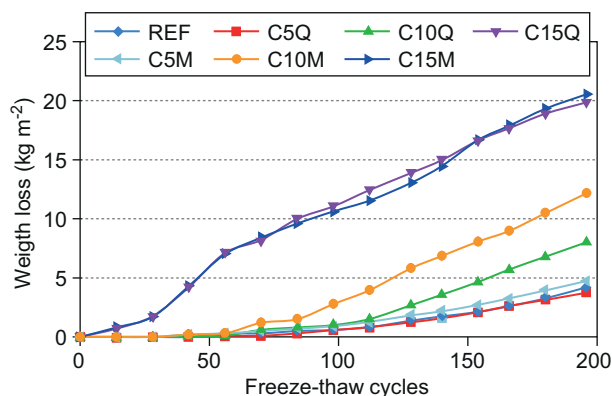
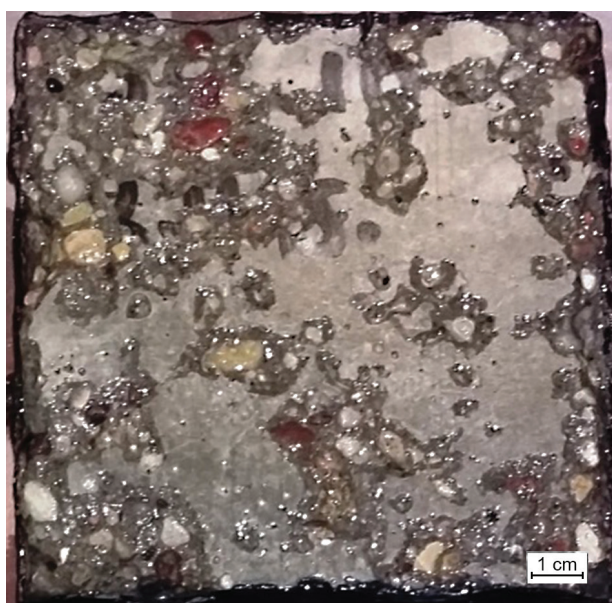


Figure 10. Surface scaling from SCC during freeze-thaw cycles.

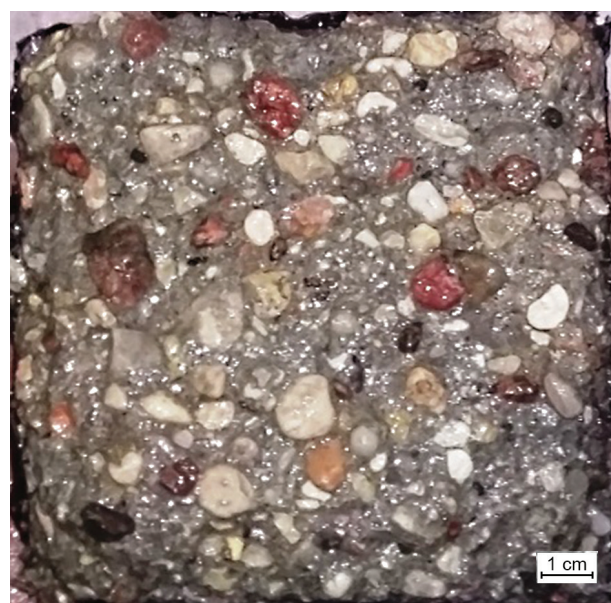
The freeze-thaw resistance was affected by the W/C ratio. The higher was the W/C in mixture composition the lower was the resistance to freeze-thaw durability. The critical W/C increase was above 0.42, when dramatic durability loss due to freeze-thaw resistance was observed (mixtures C15Q and C15M with W/C 0.45). W/C 0.40 (C5Q and C5M) and 0.38 (REF) proved to be with increased freeze-thaw durability. The freeze-thaw durability also could be attributed to the open porosity results of SCC (Table 7). The C5Q had the lowest open porosity (9.5 vol. %), which contributes to the water intake volume in the structure of SCC during freezing. While open porosity of REF was 10.7 vol. %, the low W/C and higher compressive strength ensures resistance



b) C10Q



a) C5Q



c) C15Q

Figure 11. Typical surface scaling from SCC samples after 140 freeze-thaw cycles (*continue on next page*).



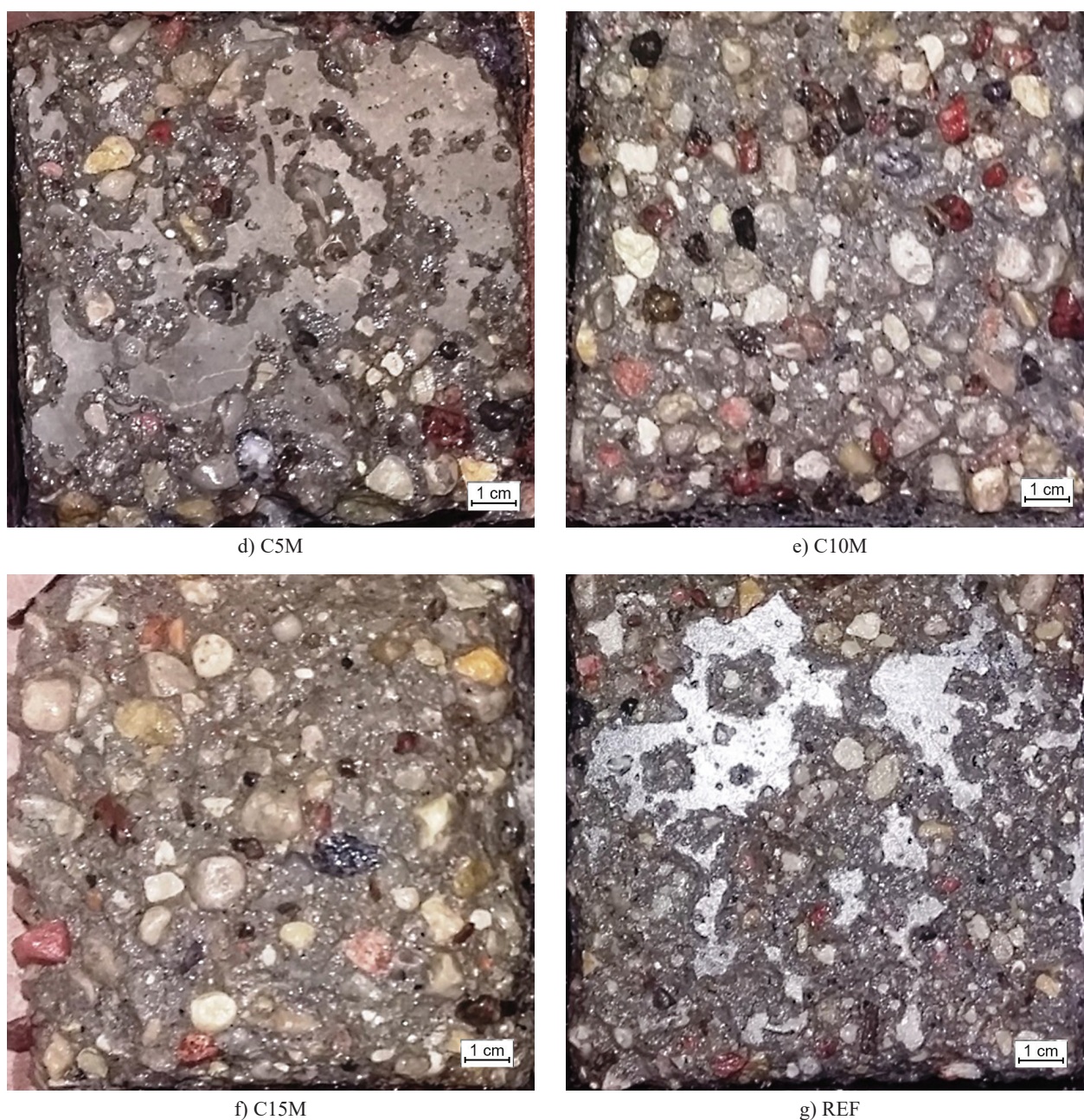


Figure 11. Typical surface scaling from SCC samples after 140 freeze-thaw cycles.

to freeze-thaw cycles. Therefore, the combination of W/C, open porosity and compressive strength of SCC determines resistance to the surface scaling and concrete deterioration during freezing and thawing.

#### Resistance to chloride penetration

SCC durability regarding to chloride penetration reduced almost in all cases when cement was partially replaced with disintegrated sand (Table 8). For REF mixture composition non-steady state migration coefficient was  $9.2 \times 10^{-12} \text{ m}^2 \cdot \text{s}^{-1}$ . Improvement regarding to resistance to chloride migration in the structure of SCC was detected only for C5Q with  $D_{nssm} 6.3 \times 10^{-12} \text{ m}^2 \cdot \text{s}^{-1}$  which

Table 8. Chloride penetration non steady state migration coefficient of SCC

Mixture composition	$D_{nssm}$ [ $\times 10^{-12} \text{ m}^2 \cdot \text{s}^{-1}$ ]
REF	$9.2 \pm 0.4$
C5Q	$6.3 \pm 0.9$
C10Q	$11.2 \pm 0.7$
C15Q	$10.0 \pm 0.2$
C5M	$12.9 \pm 1.2$
C10M	$15.5 \pm 1.4$
C15M	$12.2 \pm 1.2$



is associated with low open porosity. For other SCC mixtures  $D_{\text{nsm}}$  increased from  $12.2$  to  $15.5 \times 10^{-12} \text{ m}^2 \cdot \text{s}^{-1}$  for SCC made with MS and from  $10.0$  to  $11.2 \times 10^{-12} \text{ m}^2 \cdot \text{s}^{-1}$  for SCC made with QS. Depth of chloride ion penetration is given in Figure 12. While depth of penetration is affected by applied current, test duration and temperature, the penetration depth indicate the structure density and resistance to chloride ingress in the structure.

#### Environmental effect evaluation

It is estimated that the energy consumption of production of 1t of Portland cement clinker could be from

$1000$  to  $1800 \text{ kWh} \cdot \text{t}^{-1}$  depending from wet or dry process is used in production [11]. If 5 wt. % of Portland cement clinker would be replaced by disintegrated sand than 25 - 45 kWh of energy (5.0 % energy reduction) could be saved per  $1 \text{ m}^3$  of SCC without losing strength and durability properties.

#### CONCLUSIONS

Microfiller material in fraction of seconds could be obtained with median particle value from  $30.0$  to  $59.7 \mu\text{m}$  by milling natural fine sands by collision in disintegrator with  $E_s$  from  $8.4$  to  $25.2 \text{ kWh} \cdot \text{t}^{-1}$ . Obtained microfiller material characterized with BET surface area up to  $3571 \text{ cm}^2 \cdot \text{g}^{-1}$  similar to that of cement allowing to use it as microfiller in cement composites. The increase of milling  $E_s$  from  $8.4$  to  $25.2 \text{ kWh} \cdot \text{t}^{-1}$  effectively reduces coarsest particles while no evidence of mechanoactivation was detected with XRD.

By introduction of such microfillers in cement composites it was detected that the time factor of disintegrated sand application in cement mortar as 10 wt. % sand replacement has the critical impact on

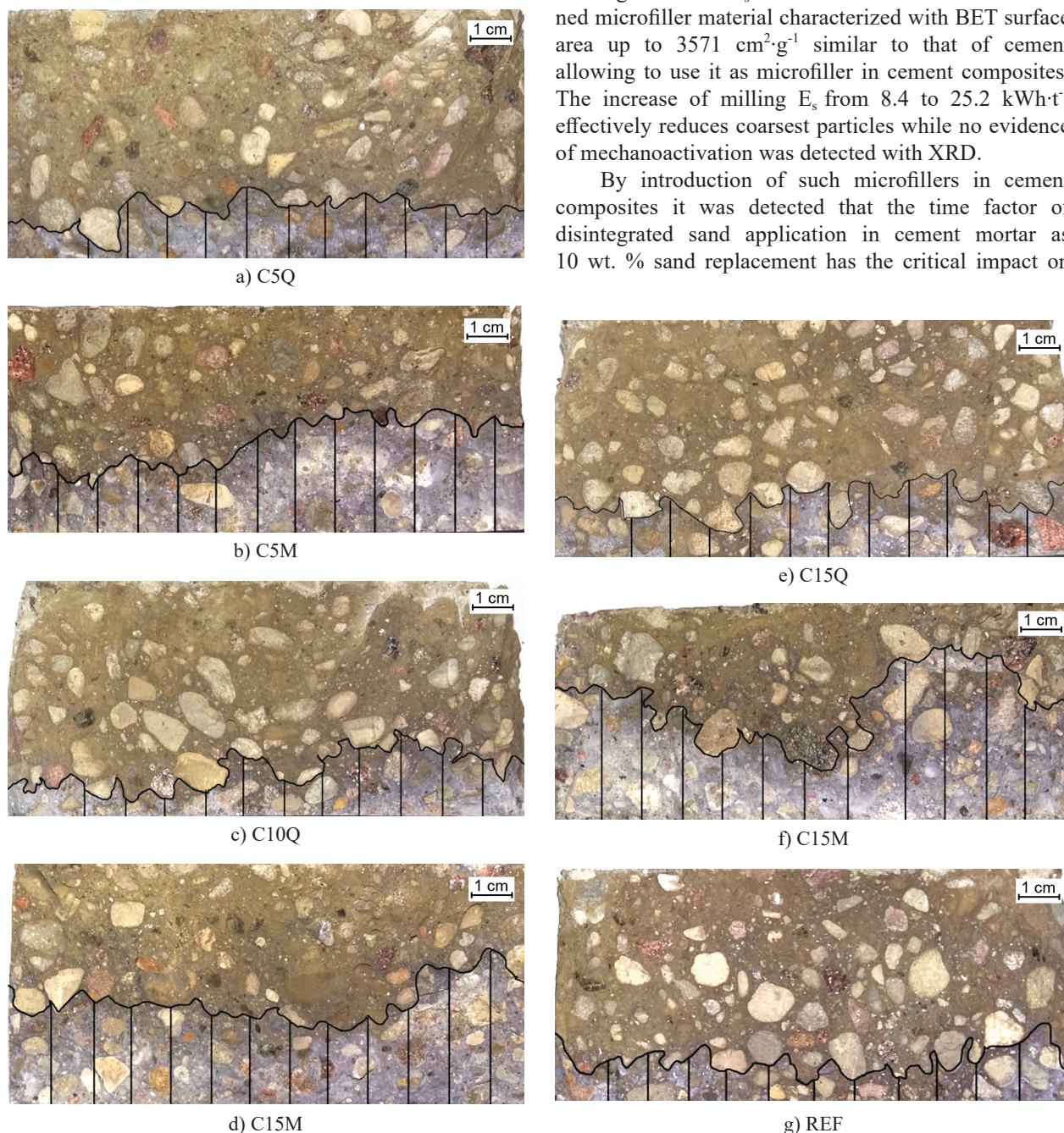


Figure 12. Split samples of SCC and determination of chloride ion penetration.

mortar compressive strength: the highest strength of cement mortar was detected if disintegrated sand was applied in mixture composition right after disintegration (strength increase up to 20 % comparing to reference). The activity of disintegrated sand decreases with time dramatically. At the age of 28 days disintegrated sand deteriorates compressive strength (from –1 to –4 %) and it was lower comparing to reference mixture.

Disintegrated sand application as partial cement replacement (up to 15 wt. %) in self-compacting concrete (SCC) reduced mechanical properties of SCC which is associated with the increase of W/C from 0.38 to 0.45. The durability of SCC regarding to freeze-thaw resistance and chloride ingress in the material structure was slightly improved by 5 wt. % partial cement replacement with disintegrated quartz sand while for other substitutions the durability of SCC reduced. The reactivity of disintegrated sand proved to be ineffective to be used as partial cement replacement in SCC due to the increase of W/C, strength and permeability of SCC.

#### Acknowledgements

Support for this work was provided by the Riga Technical University through the Scientific Research Project Competition for Young Researchers No. ZP-2016/29.

#### REFERENCES

1. Goljandin D., Kulu P., Käerdi H., Bruwier A. (2005): Disintegrator as Device for Milling of Mineral Ores. *Materials Science*, 11(4), 398-402.
2. Mehrotra S. P., Alex T. C., Greifzu G., Kumar R. (2015): Mechanical Activation of Gibbsite and Boehmite: New Findings and their Implications. *Transactions of the Indian Institute of Metals*, 69(1), 51-59. doi: 10.1007/s12666-015-0633-6
3. Nikashina V. A., Streletskii A. N., Kolbanov I. V., Meshkova I. N., Grinev V. G., Serova I. B., Shumskaya, L. G. (2011): Effect of mechanical activation on the properties of natural zeolites. *Inorganic Materials*, 47(12), 1341-1346. doi: 10.1134/S0020168511120144
4. Gbureck U. (2003): Mechanical activation and cement formation of  $\beta$ -tricalcium phosphate. *Biomaterials*, 24(23), 4123-4131. doi: 10.1016/S0142-9612(03)00283-7
5. Vdović N., Jurina I., Škapin S. D., Sondi I. (2010): The surface properties of clay minerals modified by intensive dry milling – revisited. *Applied Clay Science*, 48(4), 575-580. doi: 10.1016/j.clay.2010.03.006
6. Terada K. (2004): Physicochemical properties and surface free energy of ground talc. *Solid State Ionics*, 172(1-4), 459-462. doi: 10.1016/j.ssi.2004.03.032
7. Cao J., Fang Y., Fan R., Wan Y., Qian H., Zhou Y., Zhu W. (2015): Influence of mechanochemical effect on physical properties of boiler bottom slag. *Cailiao Kexue Yu Gongyi/ Material Science and Technology*, 23(4), 111-114. doi: 10.11951/j.issn.1005-0299.20150419
8. Pundienė I., Kligys M., Šeputytė-Jucikė J. (2014): Portland Cement Based Lightweight Multifunctional Matrix with Different Kind of Additives Containing SiO<sub>2</sub>. *Key Engineering Materials*, 604, 305-308. doi: 10.4028/www.scientific.net/KEM.604.305
9. Bajare D., Bumanis G., Upeniece L. (2013): Coal Combustion Bottom Ash as Microfiller with Pozzolanic Properties for Traditional Concrete. *Procedia Engineering*, 57, 149-158. doi: 10.1016/j.proeng.2013.04.022
10. Shakhmenko G., Korjakins A., Bumanis G. (2010). Concrete with microfiller obtained from recycled lamp glass. In: *10<sup>th</sup> International Conference Modern Building Materials, Structures and Techniques*, Vilnius Gediminas Technical University. pp. 280-284. Retrieved from <http://www.scopus.com/inward/record.url?eid=2-s2.0-84908884503&partnerID=tZOtx3y1>
11. Ohunakin O. S., Leramo O. R., Abidakin O. A., Odunfa M. K., Bafuwa O. B. (2003): Energy and Cost Analysis of Cement Production Using the Wet and Dry Processes in Nigeria. *Energy and Power Engineering*, 5, 537-550. doi: 10.4236/epe.2013.59059